Article

Periodic Tendril Perversion and Helices in the AMoOF (A = K, Rb, NH, Tl) Family

Justin C. Hancock, Matthew L Nisbet, Weiguo Zhang, P. Shiv Halasyamani, and Kenneth R. Poeppelmeier

J. Am. Chem. Soc., **Just Accepted Manuscript** • DOI: 10.1021/jacs.0c01218 • Publication Date (Web): 11 Mar 2020

Title: Periodic Tendril Perversion and Helices in the $AMoO_2F_3$ (A = K, Rb, NH_4, Tl) Family

Authors: Justin C. Hancock[1], Matthew L. Nisbet[1], Weiguo Zhang[2], P. Shiv Halasyamani[2], and Kenneth R. Poeppelmeier*[1]

[1]Department of Chemistry, Northwestern University, Evanston, Illinois 60208, United States
[2]Department of Chemistry, University of Houston, Houston, Texas, 77204, United States

Abstract

Although compounds of the formula $AMoO_2F_3$ (A = K, Rb, Cs, NH_4, Tl) have been known for decades, crystal structures have only been reported for $CsMoO_2F_3$ and $NH_4MoO_2F_3$. The three compounds $(Rb/NH_4/Tl)MoO_2F_3$ are isostructural and crystallize in the centrosymmetric space group *C*2/*c* (No. 15). The compounds contain the $MoO_2F_3^-$ anionic chain, composed of corner-sharing MoO_2F_4 octahedra, with Mo^{6+} coordinated by two *cis* bridging fluoride anions that are *trans* to terminal oxide anions. The $MoO_2F_3^-$ chain has a very unusual and complex chain structure; a single chain contains alternating zigzag and helical sections. These helical regions alternate in chirality along the chain, and thus the chains exhibit periodic tendril perversion. To the best of the authors' knowledge, no other materials with a similar chain structure have been reported. On the other hand, $KMoO_2F_3$ is noncentrosymmetric and chiral, crystallizing in the enantiomorphic space group $P2_12_12_1$ (No. 19). $KMoO_2F_3$ also contains the $MoO_2F_3^-$ anionic chain. However, the chain is helical, with only one enantiomer present, resulting in a chiral, noncentrosymmetric structure.

Introduction

Tendril perversion occurs when a helical structure contains a transitional region separating sections of opposite chirality, the prototypical example being a cucumber plant tendril or a kinked telephone cord (see Figure 1).[1] The term "helix reversal" is also used.[2] This phenomenon also occurs at the molecular level as a transition state of screw sense reversals in certain polymers such as polyacrylate and polyisocyanate.[3,4] In this case, the perversions are not static and can move along the polymer chain.[2] Tendril perversion in the crystalline solid state is rare, but it has been observed in crystals of 0D organic oligomeric foldamers.[5,6,7] It may also be possible for tendril perversion to occur at inversion twin boundaries[8], although the tendril perversion in this case would be a defect. Tendril perversion as a structural component (as opposed to a defect) appears to be unreported for inorganic materials. In this paper, we provide an atomic-scale example of tendril perversion in a family of inorganic oxyfluoride materials containing a 1D anionic chain.

Figure 1 Tendril perversion in a telephone cord. On the right side, the cord forms a right-handed helix. On the left side, it forms a left-handed helix.

Compounds exhibiting chain structural motifs feature remarkable structural diversity. Anionic chains of corner-shared octahedra ($M^{(z)}O_yF_{5-y}^{(5+y-z)-}$), where M is a transition or main group metal, z is the oxidation state of the metal, and $0 \leq y \leq 5$) are common among fluoride and oxyfluoride compounds. Compounds of the type $A_xMO_yF_{5-y}$ (x=1,2 and $0 \leq y \leq 5$), where A is a large cation such as Ba^{2+} or Cs^+, often form these anionic chains.[9] However, this stoichiometry is not required for the presence of $M^{(z)}O_yF_{5-y}^{(5+y-z)-}$, as $Pb_7V_4O_8F_{18}$ contains $VO_2F_3^{2-}$ chains.[10] The structure of the chains varies greatly. The bridging anions may be either cis ($K_2VO_2F_3$) or trans ($(NH_4)_2MoO_3F_2$) to each other, and the identity of the bridging atoms is variable in oxyfluorides.[11,12] Fluoride ions are bridging in $K_2VO_2F_3$, oxide ions are bridging in $(NH_4)_2MoO_3F_2$, and

both fluoride and oxide ions are bridging in $Pb_7V_4O_8F_{18}$.[10,11,12] The chains adopt various conformations, such as linear (K_2AlF_5), zigzag ($K_2VO_2F_3$), helical ($SrFeF_5$), and even branched (β-$BaFeF_5$).[11,13-15] In crystals with helical chains, both the right-handed and left-handed helices may be present, resulting in centrosymmetry, e.g., $SrFeF_5$, or only one enantiomer may be present, resulting in chirality, e.g., $BaAlF_5$.[16] In addition to the structural diversity among different compositions, polymorphism is also well-established among $A_xMO_yF_{5-y}$ materials.[17-19]

The oxyfluoride chain compounds $AMoO_2F_3$ (A = K, Rb, Cs, NH_4, Tl) are in the $A_xMO_yF_{5-y}$ class of materials (x = 1, y = 2). These compounds been known for over half a century, and $NH_4MoO_2F_3$ may have even been synthesized over a century ago.[20-22] Most characterization focused on Raman and IR spectroscopy.[21,23,24] A full structural analysis has only been reported for $CsMoO_2F_3$, although a partial single crystal analysis did identify the chain structure of $NH_4MoO_2F_3$.[25] The local Mo coordination is very similar for both structures; two bridging fluoride anions are *cis* with respect to each other and are *trans* with respect to terminal oxide anions. $CsMoO_2F_3$ crystallizes in the centrosymmetric space group *Imma*. The $MoO_2F_3^-$ chains form a zigzag pattern, and the Mo-F-Mo bond angles are all 180°. $NH_4MoO_2F_3$, on the other hand, is reported to crystallize in the noncentrosymmetric and enantiomorphic space group *C*2, with a more complex chain structure. The structures of $AMoO_2F_3$ (A = K, Rb, and Tl) have not been previously reported and are presented here for the first time. In addition, we report a structural solution for $NH_4MoO_2F_3$ that differs from the one previously published. A very unusual chain structure is observed in $AMoO_2F_3$ (A = Rb, NH_4, Tl). The $MoO_2F_3^-$ chains contains helical regions separated by a transitional region with linear Mo-F-Mo bonds. The helical regions alternate in handedness along the chain; thus, the chains exhibit periodic tendril perversion. To the best of the authors' knowledge, this structural phenomenon is unique among all reported crystalline materials.

Experimental

Synthesis

Caution! Hydrofluoric acid is toxic and corrosive and must be handled using the appropriate protective gear and training.[26-28]

The $AMoO_2F_3$ compounds were synthesized via hydrothermal reactions. The starting materials were molybdenum (VI) oxide (Sigma-Aldrich, 99.5%), aqueous 48% hydrofluoric acid (Sigma-Aldrich, 99.99%), and either ammonium fluoride (Alfa Aesar, 96%), potassium fluoride (Sigma-Aldrich, 99%), rubidium fluoride (Strem, 99.8%), or thallium (I) carbonate (Aldrich, 99.99%). For the synthesis of $KMoO_2F_3$, 0.900 grams of KF and 6.000 grams of MoO_3 (1:2.7 mole ratio of K to Mo) were added along with 12 mL of aqueous 48% HF to a 23-mL Teflon-lined acid digestion vessel. The vessel was heated in an oven at 160 °C for 12 hours, then cooled to room temperature over the course of about 1 day (rate ≈ 0.1 °C/min). This resulted in large, colorless crystals of $KMoO_2F_3$ with lengths up to ~0.5 cm in a 34% yield (KF basis) and no other phases. The syntheses of $AMoO_2F_3$ (A = Rb, NH_4, or Tl) were accomplished using the same temperature profile, volume of aqueous HF, and mole ratio of monovalent ion to molybdenum. Owing to the ease with which large $AMoO_2F_3$ crystals were separated from the products, no attempt was made to optimize the syntheses of $AMoO_2F_3$ for A = Rb, NH_4, and Tl. Our synthesis of $KMoO_2F_3$ resulted from exploring the possibility of making molybdenum oxide/oxyfluoride bronzes to test as magnesium battery electrodes, as magnesium has been shown to reversibly intercalate into $MoO_{2.8}F_{0.2}$.[29] However, the noncentrosymmetric, helical structure of $KMoO_2F_3$ led us to study this family of materials further.

Single crystal x-ray diffraction

Single crystal X-ray diffraction was used to determine the structure of the $AMoO_2F_3$ compounds. Crystallographic data (Table S1 and S2) and CIFs are included in the Supporting Information.

Diffraction data for $RbMoO_2F_3$, $TlMoO_2F_3$, and right-handed $KMoO_2F_3$ were collected at 100 K using a Bruker Apex II CCD diffractometer with monochromated Mo Kα (λ = 0.71073 Å) radiation. The crystal-to-detector distance was 50 mm for (Rb/Tl)MoO_2F_3 and 40 mm for $KMoO_2F_3$. SAINT V8.38A[30] was used for data integration and a multi-scan absorption correction was applied using SADABS.[31] The structure was solved using SHELXS and refined using SHELXL.[32] No additional symmetry was found when checking for higher symmetry using PLATON.[33]

Diffraction data for $NH_4MoO_2F_3$ and left-handed $KMoO_2F_3$ were collected on a Rigaku XtaLAB Synergy HyPix diffractometer with monochromated Mo Kα (λ = 0.71073 Å) radiation. The collection temperature was held at 200 K for $NH_4MoO_2F_3$ and 100 K for $KMoO_2F_3$. Data were collected at 200 K for $NH_4MoO_2F_3$ because poor refinement statistics were obtained for crystals held at 100 K when solved in the *C*2/*c* space group or the previously reported *C*2 space group. It is possible that this results from a phase transition, the nature of which is beyond the scope of this paper. While this behavior was not observed for $RbMoO_2F_3$ or $TlMoO_2F_3$, it is possible a similar phase transition occurs at temperatures below 100 K, but this possibility was not explored. The crystal-to-detector distance was 34 mm for both crystals ($NH_4MoO_2F_3$ and left-handed $KMoO_2F_3$). CrysAlisPro 1.171.40.68a was used for data integration and scaling.[34] A numerical absorption correction was applied based on gaussian integration over a multifaceted crystal model with an empirical absorption correction using spherical harmonics, as implemented in the SCALE3 ABSPACK scaling algorithm. The structure was solved using SHELXS and refined using SHELXL.[32] No additional symmetry was found when checking for higher symmetry using PLATON.[33]

Results and Discussion

$CsMoO_2F_3$

The structure of $CsMoO_2F_3$ was reported by Mattes *et al*.[21] It is discussed here as a basis for structural comparison. $CsMoO_2F_3$ crystallizes in the centrosymmetric space group *Imma*. The structure exhibits infinite chains of corner-sharing MoO_2F_4 octahedra, which are bridged exclusively by fluoride anions (see Figure 2). The bridging fluoride anions are in *cis* positions in each octahedron, and the Mo-F-Mo bond angle is 180°. Terminal oxide anions occupy the positions *trans* to the bridging fluoride anions. The molybdenum, oxygen, and bridging fluorine atoms within a chain are coplanar, resulting in a zigzag chain structure. The molybdenum octahedra are distorted; the two Mo-O bonds are the shortest (1.681(56) Å), followed by the two Mo-$F_{terminal}$ bonds (1.885(77) Å), followed by the two Mo-$F_{bridging}$ bonds (2.112 (17) Å). The one unique cesium cation is coordinated by eight anions: two equivalent oxide anions (O1) and six equivalent fluoride anions (F2). The Cs-anion distances range from 3.085(47) Å for both Cs-O bonds to 3.246(51) Å for the two long Cs-F1 bonds. The bond valence sum (BVS) for Cs using these eight bonds is 0.995. The next closest Cs-anion distance is 3.656(26) Å for Cs-O1. Considering how much larger this distance is compared with the Cs-F2 bond and the fact that each long Cs-O1 distance contributes only 0.035

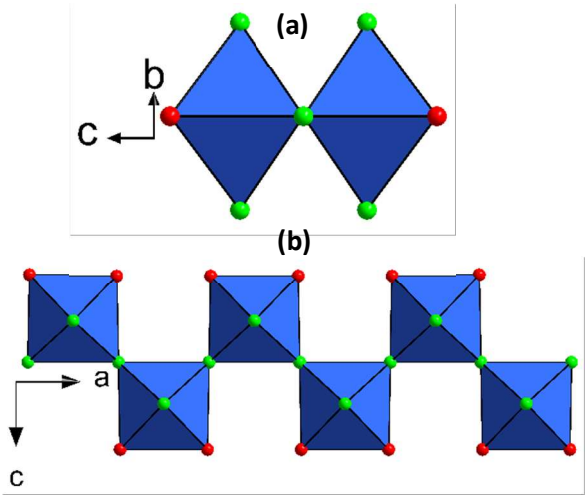

Figure 2 A fragment of the $MoO_2F_3^-$ chain in $CsMoO_2F_3$ viewed (a) along the chain axis and (b) perpendicular to the chain. Molybdenum-centered octahedra are blue, and oxygen is represented by red spheres, fluorine by green spheres.

to the BVS for Cs^+, it is appropriate to consider Cs^+ 8-coordinate. Notably, the bridging fluoride ions (F1) do not coordinate to the Cs^+ ($Cs\text{-}F_1$ distance = 3.8914(25) Å). Cesium-anion distances and bond valences are listed in Table S3.

$RbMoO_2F_3$, $NH_4MoO_2F_3$, and $TlMoO_2F_3$

$AMoO_2F_3$(A = Rb, NH_4, and Tl) are isostructural, each crystallizing in the centrosymmetric monoclinic space group *C2/c*. The crystal structure is shown in Figure 3. Our analysis is consistent with the findings of Mattes *et al*., who reported that $RbMoO_2F_3$, $NH_4MoO_2F_3$, and $TlMoO_2F_3$ shared the same powder x-ray diffraction pattern.[20] For conciseness, only $RbMoO_2F_3$ will be discussed. In $RbMoO_2F_3$, the $MoO_2F_3^-$ anion has an infinite chain structure consisting of corner-sharing MoO_2F_4 octahedra, that are bridged by fluoride anions. These chains extend along the [2 0 $\bar{2}$] direction. The local coordination of Mo is consistent with that reported for $CsMoO_2F_3$ and $NH_4MoO_2F_3$; the bridging fluoride anions are *cis* with respect to each other and *trans* to the terminal oxide anions. The molybdenum octahedra are distorted; the two Mo-O bonds are the shortest (varying from 1.6819(34) to 1.6934(30) Å), followed by the two $Mo\text{-}F_{terminal}$ bonds (varying from 1.9096(38) to 1.9251(26) Å), followed by the two $Mo\text{-}F_{bridging}$ bonds (varying from 2.1114(25) to 2.1848(25) Å). Replacement of Cs^+ with the smaller Rb^+ results in a buckling of the zigzag chain. One of the Mo-F-Mo bond angles, the Mo1-F1-Mo1 angle, remains 180°. However, the three other unique Mo-F-Mo angles are less than 180° (see Table 1). The nonlinear Mo-F-Mo bond angles result in a very unusual configuration of the $MoO_2F_3^-$ chains; the chains have chiral (helical) regions separated by a section of chain that contains a linearly-coordinated bridging fluoride (see Figure 4). The chain structure can be considered an intermediate between the zigzag chains of $CsMoO_2F_3$ and a helical chain. The helical sections between the transitional sections (the two MoO_2F_4 octahedra connected by the linearly-coordinated fluoride) nearly complete a full turn. Interestingly, the helical regions alternate in chirality along the chain, thus the chains exhibit periodic tendril perversion. We are unaware of any previous

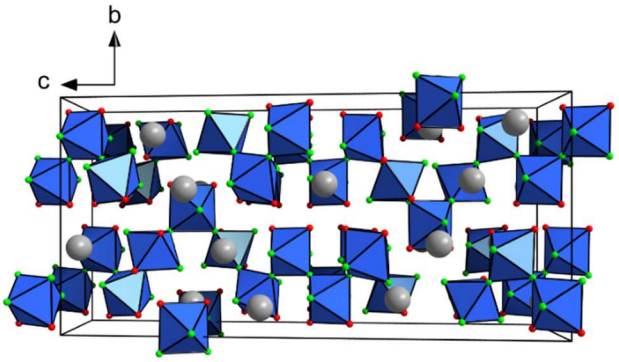

Figure 3 Crystal structure of $(Rb/NH_4/Tl)MoO_2F_3$ viewed along the a-axis. Gray, red, and green spheres represent $Rb/NH_4/Tl$, O, and F atoms, respectively. Mo octahedra are blue.

Table 1 Bond angles of bridging fluoride anions in $RbMoO_2F_3$

Atoms	Bond Angle
Mo1-F1-Mo1	180°
Mo1-F4-Mo2	157.33(12)°
Mo2-F7-Mo3	136.58(10)°
Mo3-F10-Mo4	141.31(10)°

literature on perversion in inorganic compounds, and it is possible this is the first example. If so, this is another example of a phenomenon previously only known to occur organic materials. SnIP, the structure of which was recently reported by Pfister *et al.*, is the first known example of an inorganic double helix, despite double helices being long known as the DNA structural motif.[35] The phenomenon of periodic tendril perversion along a 1D chain in $AMoO_2F_3$ (A = Rb, NH_4, Tl) appears to be unique among all crystalline materials.

In the $CsMoO_2F_3$ structure, there is only one unique Cs^+ site, as described in the previous subsection. Since $RbMoO_2F_3$ is of lower symmetry, it is not surprising that the coordination environment of Rb^+ is more complicated. Distances from Rb1 to the nearest anions vary from 2.7556(29) to 3.7505(68) Å, using the distance to the closest cation (Mo2, 3.9078(29) Å) as a cutoff. Notably, there is a large increase in the nearest anion distances between the 9th closest anion (O3, 3.1096(49) Å) and the 10th closest (O5, 3.5701(28) Å), thus it would be appropriate to consider Rb1 9-coordinate. The BVS for Rb1, assuming 9-fold coordination, is 1.26, suggesting slight overbonding. The range of the individual bond valences is 0.200 to 0.084, that suggests each of these anions should be considered coordinated to Rb1. A similar calculation is performed for Rb2 and suggests 9-fold coordination with a BVS of 1.17. There are no obvious large increases among the Rb-anion distances for Rb3 and Rb4, thus determining the coordination is less straightforward. If we consider coordinating anions only those for which the individual bond valence is greater than 0.05, then Rb3 and Rb4 are 10- and 11-coordinate, respectively. Thus, the coordination of Rb^+ in $RbMoO_2F_3$ varies and Rb^+ is on average greater than 8-coordinate, which is surprising given the smaller ionic radius of Rb^+ relative to Cs^+. However, the number of nearest anions with low BVS contributions (<0.05) does decrease. Only one anion, the bridging F1, does not coordinate to Rb^+ based on our BVS cutoff, the bridging F1, which is linearly coordinated (∠Mo1-F1-Mo1 = 180°). This is reminiscent of the $CsMoO_2F_3$ structure, in which all bridging fluorine atoms are linearly coordinated and do not coordinate to Cs^+. Rb-anion distances and BVS calculations are summarized in Table S4. Because our data was collected

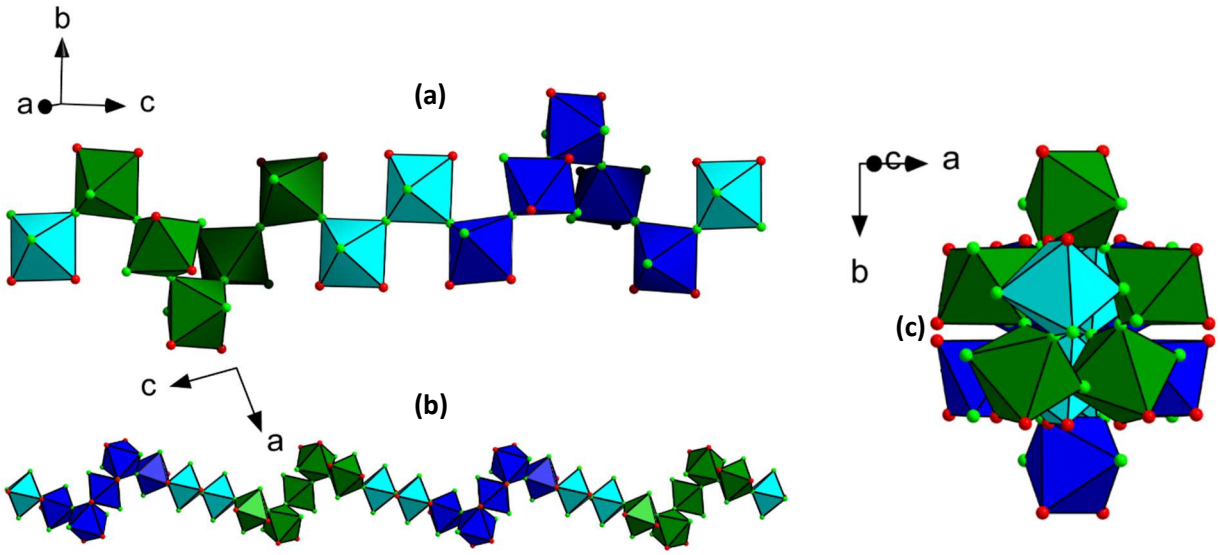

Figure 4 Views of sections of the $MoO_2F_3^-$ chain in $(NH_4/Rb/Tl)MoO_2F_3$. The green octahedra are part of a right-handed helix, the blue octahedra are part of a left-handed helix, and the cyan octahedra are the transitional region containing the two octahedra connected by a linearly coordinated fluoride. Darker octahedra are farther in the background in (a) to clarify the spacial relationships among the octahedra. Alternate views of the $MoO_2F_3^-$ chain (b) from the b direction and (c) along the chain axis, the [2 0 $\bar{2}$] direction.

at 100 K, we caution any direct bond valence comparisons between $RbMoO_2F_3$ and the room-temperature structure of $CsMoO_2F_3$.

Notably, the structure reported here for $NH_4MoO_2F_3$ is not the same as previously reported. Atovmyan *et al*. calculated a *C*2 space group for $NH_4MoO_2F_3$, with similar *a* and *b* lattice parameters, but a very different *c* lattice parameter.[25] It is possible that higher symmetry was missed, but it is also possible that $NH_4MoO_2F_3$ crystallizes in multiple polymorphs. The synthesis of $NH_4MoO_2F_3$ is not discussed in the cited article. However, it is known that the different polymorphs of α/β-$RbVOF_3$ and α/β-NH_4VOF_3 can be selectively synthesized by varying solvent systems and reaction times, respectively.[36-38] It would be of interest to apply these principles to crystallize a noncentrosymmetric polymorph, but this is beyond the scope of this study.

$KMoO_2F_3$

$KMoO_2F_3$ crystallizes in the noncentrosymmetric and chiral space group $P2_12_12_1$. The crystal structure is shown in Figure 5. The coordination of Mo and distortion of the octahedra within the $MoO_2F_3^-$ chains is very similar to that observed for $RbMoO_2F_3$; the two Mo-O bonds are the shortest (varying from 1.6827(21) to 1.6990(21) Å), followed by the two Mo-$F_{terminal}$ bonds (varying from 1.9020(17) to 1.9288(15) Å), followed by the two Mo-$F_{bridging}$ bonds (varying from 2.1061(16) to 2.2050(15) Å). However, the conformation of the chains is different; the $MoO_2F_3^-$ chains are arranged into highly irregular helices. Helices of only one handedness are present in a single crystal, and we were able to find both enantiomers in the product mixture. The chain structure is shown in Figure 6. The average Mo-F-Mo bond angle for the bridging fluorides is smaller

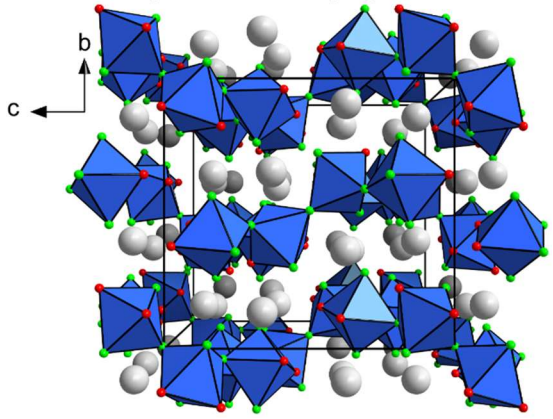

Figure 5 Crystal structure of $KMoO_2F_3$ viewed from the a-direction. Gray, red, and green spheres represent K, O, and F atoms, respectively. Mo octahedra are blue.

Table 2 Bond angles of bridging fluoride anions in $KMoO_2F_3$

Atoms	Bond Angle
Mo1-F4-Mo2	129.69(8)°
Mo2-F7-Mo3	134.88(8)°
Mo3-F10-Mo4	156.34(9)°
Mo4-F1-Mo1	130.90(8)°

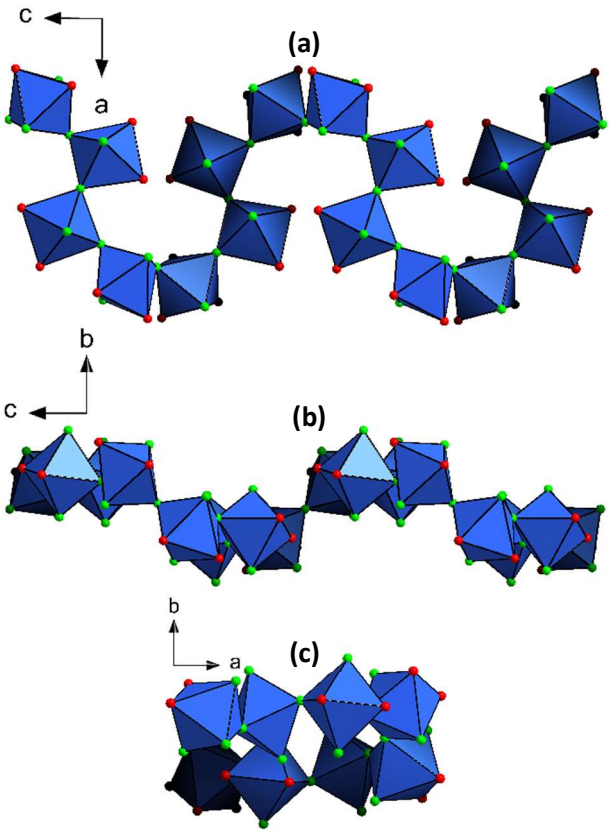

Figure 6 A view of a single $MoO_2F_3^-$ chain in $KMoO_2F_3$ viewed along the a) a-axis, b) b-axis, and c) c-axis. Gray, red, and green spheres represent K, O, and F atoms, respectively. Mo octahedra are light blue. Octahedra farther in the background have darker shading.

than $RbMoO_2F_3$ (see Table 2). This greater degree of the buckling of the chains and helicity apparently results from the smaller ionic radius of K^+ relative to Rb^+.

Even though the chains in $KMoO_2F_3$ are organized into helices of only one chirality within a crystal, tendril perversion may still be possible at inversion twin boundaries. However, the Flack parameter of both $KMoO_2F_3$ crystals examined was very close to zero: -0.004(10) and -0.003(15) for right-handed and left-handed $KMoO_2F_3$, respectively. This suggests the crystals examined were not twinned and are unlikely to have tendril perversion resulting from inversion twinning.

Helices have previously been observed to form in chains containing alternating MoO_2F_4 octahedral units and Zn/Cd-containing units, and the *cis*-directing nature of the MoO_2F_4 unit results in it being a "turning point" in the helix.[8,39,40] It is thus not surprising that a chain containing only MoO_2F_4 units can form a helix. Helical chains are known to occur in many fluorides and oxyfluorides, such as $SrFeF_5$, although the helices in $KMoO_2F_3$ are very irregular. The helix is elliptical, elongated along the a-axis (Figure 6c). The projection of the helix onto the ac plane forms an Ω-shaped wave (Figure 6a). To the best of our knowledge, this type of helix is unique among fluoride and oxyfluoride helices.

As in $RbMoO_2F_3$, the average coordination number of K^+ is greater than that of Cs^+ in $CsMoO_2F_3$. Two potassium cations are 8-coordinate, one is 9-coordinate, and one is 10-coordinate, confirmed by BVS calculations. In addition, the bridging fluoride anions do not coordinate to the alkali cation in $CsMoO_2F_3$, whereas in $KMoO_2F_3$, all of the anions coordinate to a potassium cation. Thus, replacement of Cs^+ with the much smaller K^+ results in an even greater buckling of the zigzag chain compared with replacement of Cs^+ with Rb^+, resulting in helices, but surprisingly results in a higher average coordination of the alkali cation. K-anion distances and BVS calculations are summarized in Table S5. $KMoO_2F_3$ shows second harmonic generation (SHG), consistent with a noncentrosymmetric material. The SHG efficiency of $KMoO_2F_3$ is 0.4 times that of α-SiO_2 and is not phase-matchable at 1064 nm. Experimental information (S2) and data (Figure S2) for the SHG measurements are included in the Supporting Information.

Conclusions

$CsMoO_2F_3$ was previously shown to contains anionic chains of $MoO_2F_3^-$, with corner-sharing octahedra arranged in a zigzag conformation. Replacement of Cs^+ with K^+ results in the formation of helical chains of the same handedness within a crystal and thus a noncentrosymmetric and chiral structure. Replacement of Cs^+ with Rb^+, NH_4^+, or Tl^+, which all have ionic radii in between that of Cs^+ and K^+, results in an intermediate, very unusual structure. In these compounds, the $MoO_2F_3^-$ chains contain helical sections separated by zigzag sections, and the helical regions alternate in chirality along the chains. Thus, the chains exhibit periodic tendril perversion. The authors are unaware of any other reported examples of periodic tendril perversion in 1D chains. That the structure is strongly affected by the size of the A^+ cation in $AMoO_2F_3$ suggests the possibility of engineering tendril perversion in other inorganic systems.

ASSOCIATED CONTENT

Supporting Information

Crystallographic information files (CIFs). Crystallographic tables. Tables of selected bond distances and bond valence values. Graph of SHG intensity vs. particle size. Description of stability in air. Additional experimental information.

Acknowledgements

The authors thank Charlotte Stern for helpful discussions regarding the reported crystal structures. This work was supported by the Joint Center for Energy Storage Research (JCESR), an Energy Innovation Hub funded by the U.S. Department of Energy, Office of Science, Office of Basic Energy Sciences (J.C.H. and K.R.P.). This work was also supported by funding from the National Science Foundation under grant DMR-1904701 (M.L.N.). The single crystal X-ray data measurements were acquired at Northwestern University's Integrated Molecular Structure Education and Research Center (IMSERC) at Northwestern University, which is supported by grants from NSF-NSEC, NSF-MRSEC, the KECK Foundation, the State of Illinois, and Northwestern University. PSH and WZ thank the Welch Foundation (Grant E-1457) for support.

AUTHOR INFORMATION

Corresponding Author

* Email: krp@northwestern.edu.

References

1. Gerbode, S. J.; Puzey, J. R.; McCormick, A. G.; Mahadevan, L. How the Cucumber Tendril Coils and Overwinds. *Science* **2012**, *31*, 1087-1091.

2. Nakano, T.; Okamoto, Y. Synthetic Helical Polymers: Conformation and Function. *Chem. Rev.* **2001**, *101*, 4013-4038.

3. Pietropaolo, A.; Nakano, T. Molecular Mechanism of Polyacrylate Helix Sense Switching across Its Free Energy Landscape. *J. Am. Chem. Soc.* **2013**, *135*, 5509-5512.

4. Lifson, S.; Felder, C. E.; Green, M. M. Helical conformations, internal motion, and helix sense reversal in polyisocyanates and the preferred helix sense of an optically active polyisocyanate. *Macromolecules* **1992**, *25*, 4142-4148.

5. Banerjee, A.; Raghothama, S. R.; Karle, I. L.; Balaram, P. Ambidextrous molecules: Cylindrical peptide structures formed by fusing left- and right-handed helices. *Biopolymers* **1996**, *39*, 279-285.

6. Tomsett, M.; Maffucci, I.; Le Bailly, B. A. F.; Byrne, L.; Bijvoets, S. M.; Lizio, M. G.; Raftery, J.; Butts, C. P.; Webb, S. J.; Contini, A.; Clayden, J. A tendril perversion in a helical oligomer: trapping and characterizing a mobile screw-sense reversal. *Chem. Sci.* **2017**, *8*, 3007-3018.

7. Misra, R.; George, G.; Saseendran, A.; Raghothama, S.; Gopi, H. N. Ambidextrous α,γ-Hybrid Peptide Foldamers. *Chem. Asian J.* **2019**, *14*, 4408.

8. Maggard, P. A.; Kopf, A. L.; Stern, C. L.; Poeppelmeier, K. R.; Ok, K. M.; Halasyamani, P. S. From Linear Inorganic Chains to Helices: Chirality in the $M(pyz)(H_2O)_2MoO_2F_4$ (M = Zn, Cd) Compounds. *Inorg. Chem.* **2002**, *41*, 4852-4858.

9. Leblanc, M.; Maisonneuve, V.; Tressaud, A. Crystal Chemistry and Selected Physical Properties of Inorganic Fluorides and Oxide-Fluorides. *Chem. Rev.* **2015**, *115*, 1191-1254.

10. Yeon, J.; Felder, J. B.; Smith, M. D.; Morrison, G.; zur Loye, H.-C. Synthetic strategies for new vanadium oxyfluorides containing novel building blocks: structures of V(IV) and V(V) containing $Sr_4V_3O_5F_{13}$, $Pb_7V_4O_8F_{18}$, $Pb_2VO_2F_5$, and Pb_2VOF_6. *CrystEngComm* **2015**, *17*, 8428-8440.

11. Ryan, R. R.; Mastin, S. H.; Reisfeld, M. J. The crystal structure of $K_2VO_2F_3$, a nonlinear dioxovanadium(V) group. *Acta Cryst. B* **1971**, *27*, 1270-1274.

12. Mattes, V. R.; Müller, G.; Becher, H. J. Struktur und Schwingungsspektren von Trioxodifluoromolybdaten. *Z. Anorg. Allg. Chem.* **1975**, *416*, 256-262.

13. de Kozak, A.; Gredin, P.; Pierrard, A.; Renaudin, J. The crystal structure of a new form of the dipotassium pentafluoroaluminate hydrate, $K_2AlF_5 \cdot H_2O$, and of its dehydrate, K_2AlF_5. *J. Fluorine Chem.* **1996**, *77*, 39-44.

14. von der Mühll, R.; Daut, F.; Ravez, J. Structure Cristalline de $SrFeF_5$. *J. Solid State Chem.* **1973**, *8*, 206-212.

15. von der Mühll, R.; Andersson, S.; Galy, J. Sur Quelques Fluorométallates Alcalino-Terreux. I. Structure Cristalline de $BaFeF_5$ et $SrAlF_5$. *Acta Cryst. B* **1971**, *27*, 2345-2353.

16. Domesle, R.; Hoppe, R. Zur Kenntnis von $BaAlF_5$. *Z. Anorg. Allg. Chem.* **1982**, *495*, 16-26.

17. Le Bail, A.; Mercier, A. M. Helical Octahedral *cis* Chains in α'-$BaFeF_5$. *Eur. J. Solid State Chem.* **1995**, *32*, 15-24.

18. Le Bail, A. On two new K_2FeF_5 forms. *Powder Diffr.* **2014**, *29*, 33-41.

19. Le Bail, A.; Ferey, G.; Mercier, A.-M.; De Kozak, A.; Samouel, M. Structure Determination of β- and γ-$BaAlF_5$ by X-ray and Neutron Powder Diffraction: A Model for the α→β↔γ Transitions. *J. Solid State. Chem.* **1990**, *89*, 282-291.

20. Nikolaev, N. S.; Kharitonov, Yu. Ya.; Sadikova, A. T.; Rasskazova, T. A.; Kozorezov, A. Z. Reactions of Molybdenum, Tungsten, and Uranium hexafluorides in acetic and trifluoroacetic acids. *Izv. Akad. Nauk SSSR Ser. Khim.* **1971**, *4*, 757-764.

21. Mattes, R.; Müller, G; Becher, H. J. Schwingungsspektren und Struktur von Dioxotrifluoromolybdaten und -wolframaten. *Z. anorg. allg. Chem.* **1972**, *389*, 177-187.

22. Mauro, F. Ancora sui fluossimolibdati ammonici. *Atti R. Accad. Lincei, C. Scienze FMN*. **1889**, *5*, 249-259.

23. Griffith, W. P.; Wickins, T. D. *cis*-Dioxo- and trioxo-complexes. *J. Chem. Soc. A* **1968**, 400-404.

24. Buslaev, Yu. A.; Davidovich, R. L. Infrared Absorption Spectra of Compounds of Molybdenum and Tungsten with a Bridging or an Isolated Metal-Oxygen Bond. *Russ. J. Inorg. Chem.* **1968**, *13*, 656-660.

25. Atovmyan, L. O.; Krasochka, O. N.; Rahlin, M. Ya. The Crystal Structure of Ammonium Dioxotrifluoromolybdate. *J. Chem. Soc. D* **1971**, 610-611.

26. Bertolini, J. C. Hydrofluoric acid: a review of toxicity. *J. Emerg. Med*. **1992**, *10*, 163–168.

27. Segal, E. B. First aid for a unique acid, HF: a sequel. *Chem. Health Saf*. **2000**, *7*, 18–23.

28. Peters, D.; Miethchen, R. Symptoms and treatment of hydrogen fluoride injuries. *J. Fluorine Chem*. **1996**, *79*, 161–165.

29. Incorvati, J. T.; Wan, L. F.; Key, B.; Zhou, D.; Liao, C.; Fuoco, L.; Holland, M.; Wang, H.; Prendergast, D.; Poeppelmeier, K. R.; Vaughey, J. T. Reversible Magnesium Intercalation into a Layered Oxyfluoride Cathode. *Chem. Mater.* **2016**, *28*, 17-20.

30. *SAINT V8.38A*; Bruker Analytical X-ray Instruments: Madison, WI, USA, 2016.

31. Sheldrick, G. M. *SADABS*; University of Göttingen: Göttingen, Germany, 2002.

32. Sheldrick, G. M. Crystal Structure Refinement with SHELXL. *Acta Crystallogr. Sect. C Struct. Chem.* **2015**, *71* (1), 3–8.

33. Spek, A. L. *PLATON*; Utrecht University: Utrecht, The Netherlands, 2001.

34. *CrysAlisPro* ; Rigaku Oxford Diffraction / Agilent Technologies UK Ltd, Yarnton, England, 2019.

35. Pfister, D.; Schäfer, K.; Ott, C.; Gerke, B.; Pöttgen, R.; Janka, O.; Baumgartner, M.; Efimova, A.; Hohmann, A.; Schmidt, P.; Venkatachalam, S.; van Wüllen, L.; Schürmann, U.; Kienle, L.; Duppel, V.; Parzinger, E.; Miller, B.; Becker, J.; Holleitner, A.; Weihrich, R.; Nilges, T. Inorganic Double Helices in Semiconducting SnIP. *Adv. Mater.* **2016**, *28*, 9783-9791.

36. Aldous, D. W.; Goff, R. J.; Attfield, J. P.; Lightfoot, P. Novel Vanadium (IV) Oxyfluorides with 'Spin-Ladder'-Like Structures, and Their Relationship to $(VO)_2P_2O_7$. *Inorg. Chem*. **2007**, *46*, 1277-1282.

37. Aidoudi, F. H.; Black, C.; Arachchige, K. S. A.; Slawin, A. M. Z.; Morris, R. E.; Lightfoot, P. Structural diversity in hybrid vanadium (IV) oxyfluorides based on a common building block. *Dalton Trans*. **2014**, *43*, 568-575.

38. Wustrow, A.; Hancock, J. C.; Holland, M.; Charles, N.; Rondinelli, J. M.; Poeppelmeier, K. R. Two closely related polymorphs of ammonium trifluorooxovanadate. *J. Solid State Chem.* **2019**, *276*, 261-265.

39. Maggard, P. A.; Stern, C. L.; Poeppelmeier, K. R. Understanding the Role of Helical Chains in the Formation of Noncentrosymmetric Solids. *J. Am. Chem. Soc.* **2001**, *123*, 7742-7743.

40. Ahmed, B.; Jo, H.; Oh, S.-J.; Ok, K. M. Variable Asymmetric Chains in Transition Metal Oxyfluorides: Structure-Second-Harmonic-Generation Property Relationships. *Inorg. Chem.* **2018**, *57*, 6702-6709.

TOC Graphic

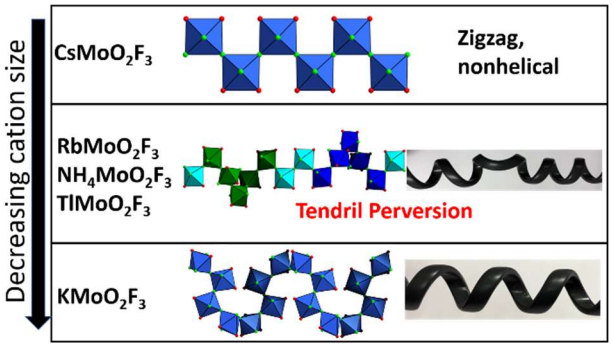
Decreasing cation size
$CsMoO_2F_3$
Zigzag, nonhelical
$RbMoO_2F_3$
$NH_4MoO_2F_3$
$TlMoO_2F_3$
Tendril Perversion
$KMoO_2F_3$